Chemical Relaxation of the Reaction of Malate Dehydrogenase with Reduced Nicotinamide Adenine Dinucleotide Determined by Fluorescence Detection*

GEORG H. CZERLINSKI AND GISELA SCHRECK†

From the Johnson Foundation, University of Pennsylvania, Philadelphia

Received July 15, 1963

Temperature-jump experiments were conducted on a system of malate dehydrogenase and DPNH between *p*H 6 and 9 and over a concentration range of two orders of magnitude. Fluorescence detection revealed a relaxation process which depends upon the concentration of the components and upon *p*H. No monomolecular interconversion was detectable. The unprotonated enzyme site reacts with DPNH with a bimolecular velocity constant of $k_4 = 6.8 \times 10^8 _{sec}{}^{-1}{}_M{}^{-1}$. The reverse monomolecular velocity constant was determined to be $k_3 = 240 _{sec}{}^{-1}$, where k_3 is the limiting value of an apparent velocity constant which is *p*H dependent. The *p*H dependence is due to the presence of a protonated enzyme-coenzyme complex with pK_H around 8 (slightly dependent upon buffer). The sum of the enthalpies of protonic dissociation of this protonated enzyme-coenzyme complex and of the dissociation of DPNH from the unprotonated complex is between −20 and −30 kcal/mole in crude approximation. The dependence of the observables upon analytical concentrations is derived.

Generally, steady-state kinetics of enzymatic reactions is able to give only two kinetic constants: one for the forward direction, one for the backward direction (except in the most elementary case, Peller and Alberty, 1959; nonreversible systems give only one kinetic constant; some multicomponent reactions may allow the determination of more than two kinetic constants, Bloomfield *et al.*, 1962a). Investigations under steady-state conditions generally do not permit one to distinguish between velocity constants as such and their combinations with equilibrium constants of adjoining rapid reactions (Bloomfield *et al.*, 1962a). Measurements under steady-state conditions also lead to Michaelis constants. Whether Michaelis constants are identical with true dissociation constants or not depends upon the ratio of the monomolecular velocity constants involved, and particularly upon the details of the reaction mechanisms. Michaelis constants of complex reaction mechanisms are rarely identical with some individual dissociation constant. Some quantitative relationships for enzyme systems with multiple intermediates in steady-state enzyme kinetics have been derived by Bloomfield *et al.* (1962a,b).

Whenever one wants to learn more than that which is accessible through steady-state kinetics, the concentration of the enzyme has to be increased (Bloomfield *et al.*, 1962a), until it, or those of its complexes with substrate or coenzyme, becomes detectable (with respect to the other components of the system). This leads immediately to higher turnover of substrates, which in turn requires rapid detection methods in order to see anything before the reaction is completed. Rapid flow methods are appropriate and have been used for kinetic investigations (Roughton and Chance, 1963). More recent methods are those of chemical relaxation (Eigen, 1954). These latter methods have several advantages over flow methods. (1) Relaxation methods are not limited by the mixing time of flow methods (around one millisecond). (2) Relaxation methods operate near equilibrium, flow methods away from it (relaxation methods may also be operated away from equilibrium by combining them with the flow method). (3) Relaxation methods employ linearized differential equations, which facilitate evaluation, especially for more complex systems. (4) The volume used per experiment can be made quite small in relaxation methods. (5) A thermodynamic parameter becomes available as by-product for each observable reaction step.

In chemical relaxation, the equilibrium constant is changed by some external parameter, such as temperature, pressure, or electric field strength. In the present temperature-jump techniques (Czerlinski and Eigen, 1959) the temperature is changed by Joule's heating: a high voltage capacitor is discharged through the electrolyte solution (the electrolysis products at the electrodes do not reach the part under observation until the measurements are completed). The product of the (ohmic) resistance of the solution and the capacitance charged gives the heating time. The energy stored on the capacitance provides the heating of the solution.

As optical detection methods are quite fast, they are most appropriate for following rapid kinetics. Most suitable for reactions involving DPNH[1] is fluorescence detection, though it requires considerable instrumental effort to obtain a fluorescent signal which is sufficiently high for rapid detection. The optical system used is shown in Figure 1 (Czerlinski, 1962). The electrodes for heating are at i, but above and below the plane of drawing. A reference channel is necessary to reduce the fluctuations of the mercury arc (differential detection). The outputs of the multiplier phototubes are connected to an oscilloscope, where the exponential change from one equilibrium value to another at higher temperature is recorded and photographed. The time constant of this curve is the (chemical) relaxation time τ.

The connection between relaxation time and velocity constants (Eigen and De Maeyer, 1963) is found by writing the differential equations for the particular mechanism. The condition of operation near equilibrium allows linearization by introducing "deviations of concentrations from their equilibrium value," Δc. This is explicitly shown in the appendix by equation (A 11); the general expression for two consecutive relaxation times is also given there by equation (A 29). Since the mathematical calculations are auxiliary to this investigation they have been placed in the appendix, but it seemed appropriate to demonstrate some general and specific derivations explicitly. This was

* Supported through grants (NSF-G-19813 and NSF-GB-237) of the National Science Foundation. The extensive support of these investigations is highly appreciated.

† Present address: Medicinska Nobelinstitutet, Biokemiska avdelningen, Solnavagen 1, Stockholm 60, Sweden.

[1] The following abbreviations are used: R = DPNH, E = active site of malate dehydrogenase, B = buffer; see Glossary.

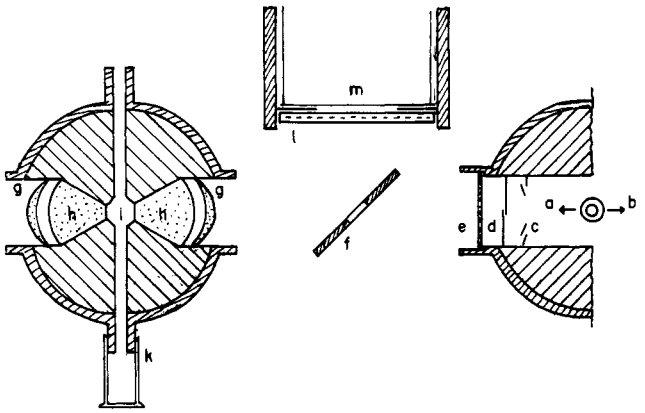

FIG. 1.—Optical system for fluorescence detection (an extended combination of Figures 8 and 12 of Czerlinski, 1962, omitting the symmetrically arranged reference part): (a) radiation of mercury arc toward test arrangement; (b) radiation of mercury arc toward reference arrangement; (c) iris diaphragm (for adjustment of light flux); (d) shutter (open only during experiment to diminish photolysis); (e) Kodak filter 18 A for fluorescence excitation (~350 mμ); (f) mirror with hole shaped like light source; side toward lamp is blackened, other side reflecting; (g) collecting lens (to diminish curvature on h); (h) conical lens, touching solution with the plane front; (i) interior of cell with enzyme system; (k) glass cylinder (tight fit) for ~2 ml volume, to fill cell (~½ ml volume); (l) Kodak Wratten filter 2B for fluorescence emission (>400 mμ); (m) front of RCA multiplier phototube, Type 2020 (selected).

necessary not only for the kinetics of chemical relaxation, but also for its "statics" and its "thermodynamics."

Theorell and Langen (1960) had demonstrated that the fluorescence of DPNH increases upon binding to malate dehydrogenase. As preliminary experiments indicated reasonably large changes upon fast temperature rises, we decided to investigate this reaction more extensively. The recent investigations of Raval and Wolfe (1962a) were helpful in setting up the experiments properly, though all later evaluations were performed without using any of their results. Our results soon revealed a two-step mechanism: a fast proton transfer reaction and a slow reaction with DPNH. In the fast step, ERH^+ *or* EH^+ could have reacted with the buffer ion B^-, while in the slow step, E *or* EH could have reacted with R. This gives four different possibilities for a two-step mechanism, written explicitly by equations (11) to (13). By thorough analysis, one possibility after the other could be excluded, until only one remained. It seemed advisable to demonstrate the analytical procedure, which resulted in a rather lengthy appendix. The evaluation resulted finally in the following scheme:

$$ERH^+ + B^- \underset{k_2}{\overset{k_1}{\rightleftharpoons}} ER + BH \qquad (1)$$

$$ER \underset{k_4}{\overset{k_3}{\rightleftharpoons}} E + R \qquad (2)$$

METHODS

The instrument was already briefly described in the introduction and was more extensively discussed by Czerlinski (1962). The temperature within the observation chamber was kept constant at 20° by cooling the electrodes with methanol. The temperature rise was determined experimentally and evaluated with derivations given formerly (Czerlinski, 1958). The *p*H indicator 4-methylumbelliferon, together with potassium phosphate or glycylglycine as buffer, was used for the determination. The temperature rise was 5°.

Malate dehydrogenase from pig heart was purchased from Boehringer over a period of several months in small samples. Each sample was dialyzed several times against K_2SO_4 of ionic strength 0.09 with phosphate buffer, *p*H 7.0, of $\mu = 0.01$. The activity of the enzyme was determined kinetically according to Ochoa (1955) and by fluorescence titration similar to a method introduced recently by Theorell and McKinley-McKee (1961) for liver alcohol dehydrogenase. An Eppendorf fluorimeter was used for this purpose, 366 mμ excitation, 411 mμ emission. A known quantity of enzyme solution was incubated with 0.04 M potassium D-malate, phosphate buffer of *p*H 7.0 and ionic strength 0.02. Small quantities of DPNH solution were added and the concentration of DPNH at the inflection point of the titration curve was taken as equivalence point for the number of enzymatically active sites.

DPNH was Sigma grade (stored dry at 4°) and its concentration was determined spectrophotometrically by measuring its absorption at 340 mμ in a 1-cm cuvet, taking 6220 M^{-1} cm^{-1} as extinction coefficient at this wavelength (Kornberg, 1953; measured immediately upon preparation and in frequent intervals thereafter).

Ordinary deionized water was redistilled in quartz under nitrogen with addition of alkaline permanganate. Ion migration out of the flask was prevented by a special sleeve heated above 100°. The purity of the distilled water was tested conductometrically (at 10 kc). The ionic strength of the solution was always adjusted to 0.1 by the addition of K_2SO_4, Baker Analyzed Reagent. The experiments were conducted either in potassium phosphate, Baker Analyzed Reagent, $\mu = 0.1$, or in glycylglycine, Nutritional Biochemical Corporation, 0.02 M. The *p*H was checked with a Radiometer *p*H Meter 22.

GLOSSARY

In order to facilitate reading of the text, a glossary of symbols will be given first.

Y Generalized individual component in a biochemical system, here Y = E, R, ER, ERH, B, BH, H, which are generally ions, but the charges have been omitted for simplicity. H = hydrogen ion, B = unprotonated buffer, R = DPNH, and E = active site of the enzyme; combined letters describe associated components.

Z Used like Y when more than one generalized individual component has to be considered.

S_0 Background fluorescence; the residual signal [in mv] obtained without R being present in the setup of Figure 1. It is near 500 mv with 0.1 megohm load resistor at the anode of the multiplier phototube.

S_T Total fluorescence signal [in mv] obtained with the complete biochemical system; same conditions as for S_0.

S_Y Fluorescence signal obtained from component Y only.

ΔS_T Momentary change in the total fluorescence signal, which includes all components; compare equation (3).

ΔS_Y Momentary change in the fluorescence signal from component Y, given in mv.

$\Delta \bar{S}_Y$ Equilibrium change in the fluorescence signal of component Y, in mv.

$\Delta \bar{S}_0$ Total change in the fluorescence signal due to the change in fluorescence yield of all components upon raising the temperature from 20° to 25°.

$\Delta \bar{S}_j$ With $j \geq 1$ is the total change in the fluorescence signal due to the change in the concentrations of all components caused by the *j*th relaxation process; compare equation (A 50).

τ Chemical relaxation time, referring to a system with only one relaxation time; otherwise an index *j* indicates

the number of the relaxation time; index zero refers to the heating time constant.

η_Y Molar fluorescence coefficient of component Y, given in mv per μM.

k_m Velocity constant of an individual reaction step in the direction given by the arrow, associated to it and in the symbolism of chemical reaction steps (see equations 1 and 2.)

$K_{m,m+1}$ Equilibrium constant of an individual reaction step with m and $m + 1$ indicating the indexing of the associated velocity constants; see for instance equation (17).

$K_{Y,Z}$ Dissociation constant of the association product YZ, dissociating into the individual components Y and Z, equation (17) or (21).

K_0 Complex dissociation constant, introduced for simplifying some expressions. It is here a pH-dependent dissociation constant with all four simple cases being considered, equation (16).

$\Delta K_{Y,Z}$ Change in the equilibrium constant $K_{Y,Z}$ due to the temperature jump of 5°.

$\Delta H_{Y,Z}$ Change in enthalpy of the reaction step, described by $K_{Y,Z}$ for 23°, in kcal per mole.

c_Y Momentary concentration of component Y, which changes with time.

c_Y^0 Analytical concentration of component Y; all equilibrium concentrations are added together in which component Y appears as such *or* in combinations, see equations (A 2) and (A 3).

$\bar{c}_Y$ Concentration of component Y present at equilibrium in the complete biochemical system, given in μM (or in M); $t = 20°$ for statics.

Δc_Y Momentary deviation in the concentration of component Y from the equilibrium value *after* the temperature jump of 5°, that is, at 25°; see equation (A 11).

$\Delta\bar{c}_Y$ Total change of the equilibrium concentration of the component Y from *before* the temperature jump to thereafter for the general case that all chemical relaxation processes are finished; see equation (A 53).

$(\Delta\bar{c}_Y)_j$ Total change of the equilibrium concentration of component Y *up to and including* the jth relaxation process. For their relation to concentration changes of *individual* relaxation processes it is referred to equations (A 65) to (A 67) and their discussion.

A_{ij} Equilibrium concentration [in M or in μM], referring to that component Y which was selected as the ith concentration variable in the system of differential equations and which is associated with the jth relaxation time. Compare equation (A 25) to (A 27).

a_{ij} Coefficient of time constants [in sec^{-1} or $msec^{-1}$], referring with i to that component Y which was selected as the ith concentration variable in the system of differential equations. The second index, j, refers to any one component, the concentration of which was selected as variable in the system of differential equations.

b Dimensionless parameter in the solution of differential equations; equation (A 30).

α, β, γ Dimensionless parameters used to simplify a complex expression; equation (41).

Results

Initial experiments were carried out at pH 7.0 in phosphate buffer. A typical experiment is shown in Figure 2. The initial part of the horizontal trace (about 2 cm) indicates the equilibrium position before the temperature jump (that is, at 20°), while its final horizontal part (last 2 cm) indicates the new equilibrium position (that is, at 25°). The temperature jump occurs "instantaneously" for the deflection time of the oscilloscope beam, namely, at the stepwise change in the vertical position. The stepwise change is followed by an exponential one, which actually indicates the chemical relaxation. The very fast initial change is due to the change of fluorescence yield with temperature, concurrent with the heating process.

The total change of fluorescence signal with time,

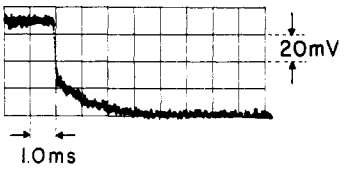

FIG. 2.—Oscillograph trace of a mixture of malate dehydrogenase with DPNH, both in equal amounts at 6 μM in phosphate, pH 7.0, ionic strength 0.1. Electronic RC filter set at 0.95 μsec, horizontal deflection 1.0 msec/cm, vertical deflection 20 mv/cm.

ΔS_T, is described for a system with two *separated* chemical time constants τ_1 and τ_2 by

$$\Delta S_T = \Delta\bar{S}_0 \exp(-t/\tau_0) + \Delta\bar{S}_1 \exp(-t/\tau_1) + \Delta\bar{S}_2 \exp(-t/\tau_2) \quad (3)$$

Figure 3 represents equation (3) on a semilog plot, where τ_0 is the heating time constant in an RC-discharge circuit defined by $^1/_2$ RC; ΔS_0 would then be due to the change of the signal from components, which as such demonstrates temperature dependence of fluorescence. This is true for components with lower fluorescence yield, demonstrating a change in yield with temperature. Here $\Delta\bar{S}_1$ and $\Delta\bar{S}_2$ are time-independent fluorescence signal changes associated with chemical time constants τ_1 and τ_2, respectively.

In an actual experiment, like that of Figure 2, conditions frequently do not permit telling in advance how many time constants are hidden in the initial step. One therefore assumes initially no *chemical* time constant and tries to find expressions for the experimental results. In order to obtain information on the chemistry of this relaxation process, the reciprocal of the relaxation time has to be plotted as a function of concentration. The upper and lower limits of relaxation times were obtained as explained previously by Czerlinski and Schreck (1964).

In the initial approach, one has to consider the following two reaction schemes for the combination of the active site of malate dehydrogenase with reduced DPNH:

$$E + R \underset{k_2}{\overset{k_1}{\longleftrightarrow}} ER \quad (4)$$

$$E + R \underset{k_2}{\overset{k_1}{\longleftrightarrow}} ER \underset{k_4}{\overset{k_3}{\longleftrightarrow}} EX \quad (5)$$

If $\bar{c}_Y$ represents the equilibrium concentration of any component Y, one obtains for scheme (4):

$$\tau_1^{-1} = k_1(\bar{c}_E + \bar{c}_R) + k_2 \quad (6)$$

Scheme (5) would result in two different relaxation times. If the left-hand reaction is much faster than the right-hand one, the fast relaxation time would follow equation (6), while the slow one would follow

$$\tau_2^{-1} = k_4 + k_3 \frac{\bar{c}_E + \bar{c}_R}{K_{2,1} + \bar{c}_E + \bar{c}_R} \quad (7)$$

where the dissociation constant $K_{2,1} = k_2/k_1$. A derivation of these equations will not be given here.[2]

If the right-hand reaction is much faster than the left-hand one, the reciprocal of the fast relaxation time would consist of the sum of the velocity constants of this reaction, $\tau^{-1} = k_3 + k_4$; the slow relaxation time

[2] Equations of these types have been derived formerly, originally by Eigen (1954), who recently published a more general treatment (Eigen and De Maeyer, 1963). Recently we showed the derivation of the equations for a scheme like equation (5) in another context (Czerlinski and Schreck, 1964).

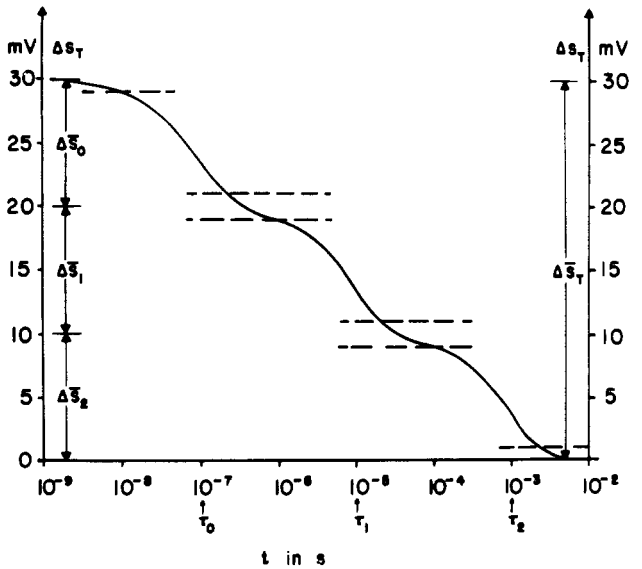

FIG. 3.—Representation of equation (3) with logarithmic abscissa and $\tau_0 = 10^{-7}$ sec, $\tau_1 = 10^{-5}$ sec, $\tau_2 = 10^{-3}$ sec, $\Delta\bar{S}_0 = \Delta\bar{S}_1 = \Delta\bar{S}_2 = 10$ mv. The dashed lines in the graph represent ± 10% error limit in ΔS_j.

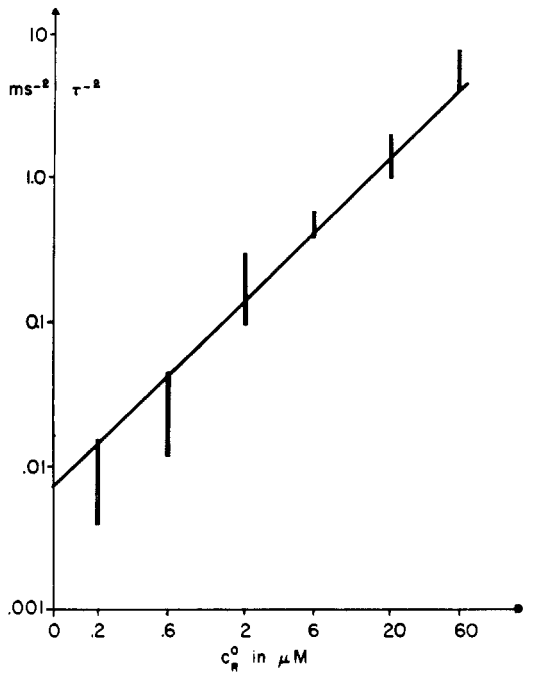

FIG. 4.—Demonstrates a plot of the experimental τ^{-2} as a function of the initial concentration of DPNH. The straight line follows equation (9) with $k_2 = 45$ sec^{-1} and $k_1 = 6.8 \times 10^8$ sec^{-1} M^{-1}.

would not be experimentally distinguishable from equation (6), though k_2 would also contain k_3 and k_4. High $\bar{c}_R$ would allow an experimental distinction between (6) and (7): τ^{-1} would become proportional to $\bar{c}_R$ according to (6), while it would reach a constant value according to (7). Figure 4 shows that the curve does not bend over: (7) is not valid; but as Figure 4 demonstrates $\tau^{-2} = f(c_R{}^0)$, this reasoning is only qualitative. If no equilibrium data should be taken from the literature, one has to express τ as a function of total concentrations. If $c_E{}^0 = c_R{}^0$, then $\bar{c}_E = \bar{c}_R$ also and

$$\bar{c}_R = -\frac{K_{2,1}}{2}\left[1 - \left(1 + \frac{4c_R{}^0}{K_{2,1}}\right)^{1/2}\right] \qquad (8)$$

Though its specific derivation is omitted here (see Czerlinski and Schreck, 1964), similar equations are used later on in the appendix. One may now combine (6) with (8) and obtains after simplification and squaring:

$$\tau^{-2} = k_2{}^2 + 4k_1k_2c_R{}^0 \qquad (9)$$

To present the broad range in τ^{-2} and $c_R{}^0$, a log-log plot is necessary and given for some data in Figure 4. The theoretical curve in this figure is obtained with equation (9), $k_2 = 45$ sec^{-1} and $k_1 = 6.8 \times 10^8$ sec^{-1} M^{-1}.

Experiments were then conducted to investigate the influence of other ionic compounds. For this purpose two different buffers were used at various *p*H values. The results indicated clearly a *p*H dependence of the reaction. The simplest representation would be obtained by two consecutive reactions, a fast one, describing the proton transfer, and a slow one, describing the combination with DPNH. The system actually allows four different possibilities for such a combination, namely:

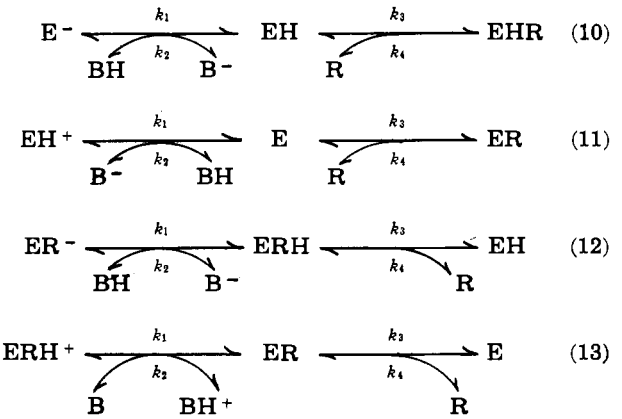

In these four schemes B is buffer, which is present at much higher concentration than free H^+, so that the enzyme would react with the appropriate form of the buffer. Application of the mathematical methods of chemical relaxation (shown in the appendix only for the system of equation 13) lead to various equations for the four systems (10) to (13), which will now be summarized under the headings Statics and Kinetics.

Statics.—Statics represents the description of the total fluorescence signal S_T in terms of equilibrium constants and initial concentrations $c_Y{}^0$. S_0 is the fluorescence signal without DPNH and η_Y is the "molar fluorescence coefficient of component Y," given in mv μM^{-1} (or similar units; it is dependent upon many instrumental conditions, see Czerlinski, 1962).

System (10):

$$S_T - S_0 = \eta_{EHR}c_R{}^0 + (\eta_R - \eta_{EHR})\bar{c}_R \qquad (14)$$

where

$$\bar{c}_R = -\frac{K_0}{2}\left\{\left[1 + \frac{4c_R{}^0}{K_0}\right]^{1/2} - 1\right\} \qquad (15)$$

$$K_0 = K_{EH,R}\frac{\bar{c}_H + K_{E,H}}{\bar{c}_H} \qquad (16)$$

$$K_{EH,R} = \frac{\bar{c}_{EH}\bar{c}_R}{\bar{c}_{EHR}} = K_{4,3} = \frac{k_4}{k_3} \qquad (17)$$

$$K_{E,H} = \frac{\bar{c}_E\bar{c}_H}{\bar{c}_{EH}} = K_{2,1}K_{B,H} = \frac{k_2}{k_1}\cdot\frac{\bar{c}_B\bar{c}_H}{\bar{c}_{BH}} \qquad (18)$$

System (11):

$$S_T - S_0 = \eta_{ER}c_R{}^0 + (\eta_R - \eta_{ER})\bar{c}_R \qquad (19)$$

where $\bar{c}_R$ follows equation (15), but

$$K_0 = K_{E,R}\frac{K_{E,H} + \bar{c}_H}{K_{E,H}} \quad (20)$$

$$K_{E,R} = \frac{\bar{c}_E\bar{c}_R}{\bar{c}_{ER}} = K_{4,3} = \frac{k_4}{k_3} \quad (21)$$

$$K_{E,H} = \frac{\bar{c}_E\bar{c}_H}{\bar{c}_{EH}} = \frac{K_{B,H}}{K_{2,1}} = \frac{K_{B,H}k_1}{k_2} \quad (22)$$

Here $K_{E,H}$ has the same definition in terms of concentrations as in equation (18), but the relation to the velocity constants is different due to the different sequence in the chemical equations.

System (12):

$$S_T - S_0 = \eta_{ERH}c_R^0 + (\eta_{ER} - \eta_{ERH})\bar{c}_{ER} + (\eta_R - \eta_{ERH})\bar{c}_R \quad (23)$$

where

$$\bar{c}_R = \frac{K_0}{2}\left\{\left[1 + \frac{4c_R^0}{K_0}\right]^{1/2} - 1\right\} \quad (24)$$

$$K_0 = K_{EH,R}\frac{\bar{c}_H}{\bar{c}_H + K_{ER,H}} \quad (25)$$

$$K_{EH,R} = \frac{\bar{c}_{EH}\bar{c}_R}{\bar{c}_{EHR}} = K_{4,3}^{-1} = \frac{k_3}{k_4} \quad (26)$$

$$K_{ER,H} = \frac{\bar{c}_{ER}\bar{c}_H}{\bar{c}_{ERH}} = K_{2,1}K_{B,H} \quad (27)$$

$$\bar{c}_{ER} = c_R^0\left\{1 + \frac{\bar{c}_H}{K_{ER,H}}\left(1 + \frac{K_{EH,R}}{2c_R^0}\right)\right\}\left(1 + \frac{\bar{c}_H}{K_{ER,H}}\right)^{-2}\left\{1 - \left[1 - \frac{\left(1 + \frac{\bar{c}_H}{K_{ER,H}}\right)^2}{\left\{1 + \frac{c_H}{K_{ER,H}}\left(1 + \frac{K_{EH,R}}{2c_R^0}\right)\right\}^2}\right]^{1/2}\right\} \quad (28)$$

System (13):

$$S_T - S_0 = \eta_{ERH}c_R^0 + (\eta_{ER} - \eta_{ERH})\bar{c}_{ER} + (\eta_R - \eta_{ERH})\bar{c}_R \quad (29)$$

$$\bar{c}_R = \frac{K_0}{2}\left\{\left[1 + \frac{4c_R^0}{K_0}\right]^{1/2} - 1\right\} \quad (30)$$

$$K_0 = K_{E,R}\frac{K_{ER,H}}{K_{ER,H} + c_H} \quad (31)$$

$$K_{E,R} = \frac{\bar{c}_E\bar{c}_R}{c_{ER}} = K_{4,3}^{-1} \quad (32)$$

$$K_{ER,H} = \frac{\bar{c}_{ER}\bar{c}_H}{\bar{c}_{ERH}} = \frac{K_{B,H}}{K_{2,1}} \quad (33)$$

$$\bar{c}_{ER} = c_R^0\frac{K_{ER,H}}{K_{ER,H} + \bar{c}_H}\left\{1 + \frac{K_0}{2c_R^0}\right\}\left\{1 - \left[1 - \left(1 + \frac{K_0}{2c_R^0}\right)^{-2}\right]^{1/2}\right\} \quad (34)$$

Kinetics.—Kinetics describes the relationships between the measured relaxation times and the velocity constants of the system. The protonic conversions are considered here "immeasurably fast" and are contained in the initial stepwise rise (as far as they appear in fluorescence). Only the slower combination with DPNH is therefore described.

System (10):

$$\tau_2^{-2} = k_4^2 + 4c_R^0k_4k_3\frac{\bar{c}_H}{\bar{c}_H + K_{E,H}} \quad (35)$$

System (11):

$$\tau_2^{-2} = k_4^2 + 4c_R^0k_4k_3\frac{K_{E,H}}{K_{E,H} + \bar{c}_H} \quad (36)$$

System (12):

$$\tau_2^{-2} = \left(k_3\frac{\bar{c}_H}{\bar{c}_H + K_{ER,H}}\right)^2 + 4c_R^0k_4k_3\frac{\bar{c}_H}{\bar{c}_H + K_{ER,H}} \quad (37)$$

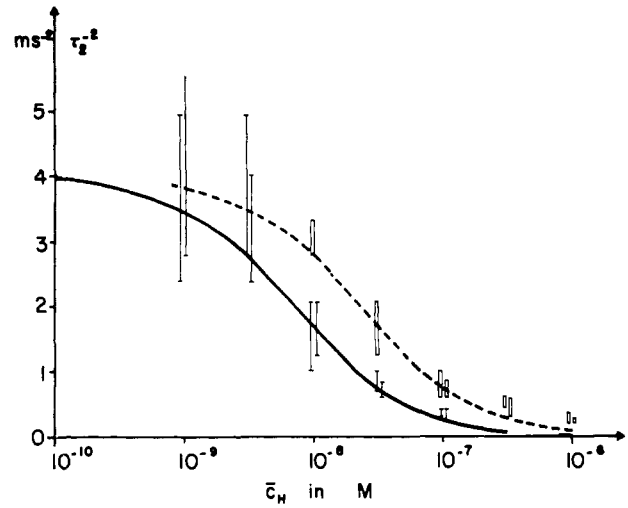

FIG. 5.—Plot of τ_2^{-2} as a function of $\bar{c}_H$ at $c_R = 6$ μM. The rectangular boxes represent, as in former drawings, phosphate buffer, while the vertical lines represent glycylglycine buffer; K_2SO_4 always added to ionic strength 0.1.

System (13):

$$\tau_2^{-2} = \left(k_3\frac{K_{ER,H}}{\bar{c}_H + K_{ER,H}}\right)^2 + 4c_R^0k_4k_3\frac{K_{ER,H}}{K_{ER,H} + \bar{c}_H} \quad (38)$$

There are now two equations available for each one of four possible combinations of the two reactions. Figure 5 demonstrates a plot of $\tau_2^{-2} = f(\bar{c}_H)$ at $c_R^0 = 6$ μM. Theoretical lines have been drawn (to be discussed later),[3] which have their inflection points around *p*H 8. In a preliminary investigation, therefore, 8 may be considered as the pK_H of the enzyme (-complex). Comparing equation (9) with (35) to (38) gives immediately the relationships between the velocity constants. So, for instance, for (35): k_4 = [k_2 of equation (9)]

$$k_3\frac{\bar{c}_H}{c_H + K_{E,H}} = [k_1 \text{ of equation (9)}] \quad (39)$$

or for (38), which will be used mainly later on: k_4 = [k_1 of equation (9)] and

$$k_3\frac{K_{ER,H}}{c_H + K_{ER,H}} = [k_2 \text{ of equation (9)}] \quad (40)$$

One obtains then for system (13): $k_4 = 6.8 \times 10^8$ sec^{-1}-M^{-1} = 0.68 msec$^{-1}\mu$M^{-1} and $k_3 = 240$ sec^{-1} = 0.24 msec^{-1} as [k_2 of equation (9)] = 45 sec^{-1}. The remaining values are shown in the legend to Figure 6, which demonstrates the theoretical curves for the four different cases of (35) to (38). It becomes immediately apparent that only equations (11) and (13) could describe the experimental results.

After kinetic data have been evaluated, all equilibrium parameters are available to employ equations (14), (19), (23), and (29). Calibration experiments led to η_R = 65 mv/μM. Later evaluation led to an upper limit in the molar fluorescence coefficient of bound DPNH, namely 170 mv/μM. This is set for η_{EHR} in (14) and for η_{ER} in (19). In equations (23) and (29) there are two alternatives, and one can not determine in advance the highest molar fluorescence coefficient. Figure 7 demonstrates the experimental results, showing that η_{ERH} is largest (= 170 mv/μM). One may

[3] Equations (35) to (38) contain certain simplifications, which will be discussed in the appendix when and after (38) is derived. Similar simplifications apply to the derivations of the other equations.

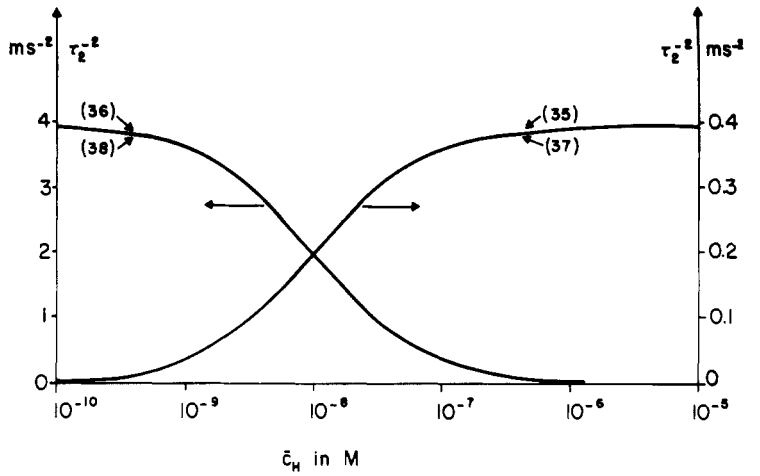

FIG. 6.—Theoretical curves of τ_2^{-2} as a function of $\bar{c}_H$ for four different cases of combinations of a protonic reaction with an association reaction of enzyme with coenzyme. The numbers within the graph refer to equation numbers of the main text. A horizontal arrow next to a curve indicates the ordinate which must be considered for this relaxation.

then derive tentatively from the lower limit:[4] $\eta_{ER} = 83$ mv/μM. These latter two values for molar fluorescence coefficients are taken for both equations (23) and (29). Theoretical curves may now be drawn for all possibilities, as is shown in Figure 8.

By comparison of the last four figures one may conclude: System (10) is not possible, as equation (35) does not represent the experimental results of Figure 5. System (11) has no reality, as equation (19) is not a representation of the results of Figure 7. System (12) can not be considered, as equation (37) is not a representation of the data of Figure 5. Only system (13) fulfills the experimental results with all equations: equation (38) represents the theoretical curve in Figure 5 and equation (29) the theoretical curve in Figure 7.

Because of the importance of equation (29), it may be written more explicitly by combining (29) to (34). It is then:

$$\frac{S_T - S_0}{\eta_R c_R^0} = 1 + [\alpha + \beta]\gamma \qquad (41)$$

where

$$\alpha = \left(\frac{\eta_{ERH}}{\eta_R} - 1\right) \frac{\bar{c}_H}{\bar{c}_H + K_{ER,H}} \qquad (42)$$

and

$$\beta = \left(\frac{\eta_{ER}}{\eta_R} - 1\right) \frac{K_{ER,H}}{K_{ER,H} + \bar{c}_H} \qquad (43)$$

while

$$\gamma = \left\{1 + \frac{K_{E,R}}{2c_R^0} \cdot \frac{K_{ER,H}}{K_{ER,H} + \bar{c}_H}\right\} \left\{1 - \left[1 - \left\langle 1 + \frac{K_{E,R}}{2c_R^0} \cdot \frac{K_{ER,H}}{K_{ER,H} + \bar{c}_H} \right\rangle^{-2}\right]^{1/2}\right\} \qquad (44)$$

Considering the limits, one finds for

$$\bar{c}_H \ll K_{ER,H}: \quad \alpha \to 0 \quad \text{and} \quad \beta \to \frac{\eta_{ER}}{\eta_R} - 1$$

$$\bar{c}_H \gg K_{ER,H}: \quad \alpha \to \frac{\eta_{ERH}}{\eta_R} - 1 \quad \text{and} \quad \beta \to 0$$

For the latter case, $\gamma \to 1$.
For $\bar{c}_H \lesssim K_{ER,H}$, one may consider

$$2c_R^0 \ll K_{E,R}, \quad \text{then} \quad \gamma \to \frac{c_R^0}{K_{E,R}} \cdot \frac{K_{ER,H} + \bar{c}_H}{K_{ER,H}}$$

$$2c_R^0 \gg K_{E,R}, \quad \text{then} \quad \gamma \to 1.$$

[4] The evaluations are easily visible for the case of system (13), where (41) gives the full description and limits are actually considered after equation (44).

Though it is in zero-approximation $K_{ER,H} = 10^{-8}$ M, the experimental data in Figure 7 show for the inflection point differences which seem to justify the determination of separate $K_{ER,H}$, leading to buffer-dependent dissociation constants. The best fit appears to be for phosphate: $K_{ER,H} = 2.3 \times 10^{-8}$ M, and for glycylglycine: $K_{ER,H} = 0.7 \times 10^{-8}$ M; the former value leads to $k_3 = 240$ sec^{-1}. These are the parameters which have been used for the theoretical curves in Figure 5 (and in Figure 7).

Experiments have also been conducted with c_R^0 as independent variable at different pH values. The results are summarized in Figure 9. The theoretical curves were drawn with the above parameters and the appropriate $\bar{c}_H$. Unfortunately, only poor precision is obtainable. Only the trend of the dependence could be seen from the experimental data. This aspect will be considered again under Discussion.

Thermodynamics.—Figures 10 and 11 give the total signal changes as derived from chemical relaxation.

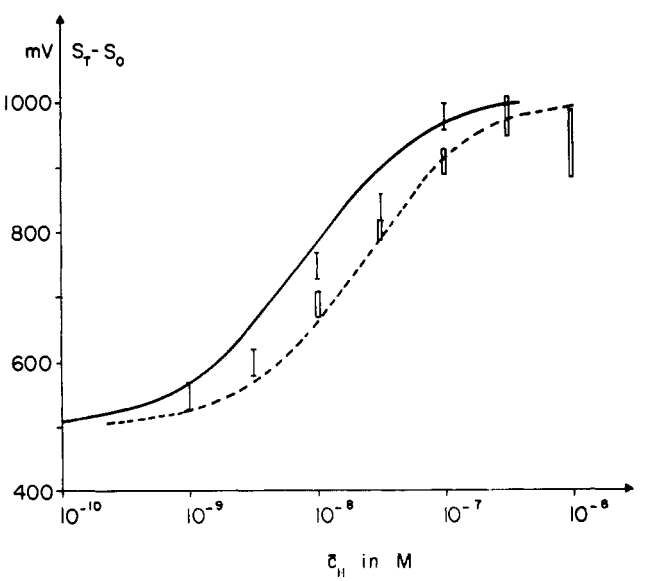

FIG. 7.—A plot of the experimental results of the total chemical signal $S_T - S_0$ as a function of $\bar{c}_H$, vertical boxes refer to phosphate, vertical lines to glycylglycine as buffer. The dashed curve is inserted with the kinetically derived constants for phosphate, while the solid line is inserted with the kinetically derived constants for glycylglycine as buffer.

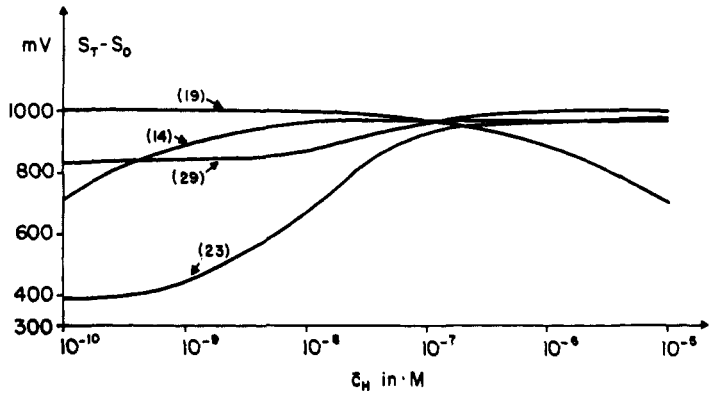

FIG. 8.—Theoretical curves for four cases where the numbers indicate the equations of the main text. These theoretical curves are for the purpose of distinguishing between various types of reactions.

Although the theory is briefly derived in the appendix, the crudeness of the results does not warrant inserting thoeretical curves into the graphical representations. A highly simplified description is given by a combination of (A 64) with (A 67)

$$\Delta\bar{S}_2 \approx \eta_{ERH} \frac{\Sigma\Delta H}{1+p} \cdot \frac{\Delta T}{RT^2} \bar{c}_{ERH} \qquad (45)$$

where $\Delta\bar{S}_2$ is the actually observed change in mv and $\Sigma\Delta H$ is the effective sum of the individual enthalpies in the reaction. Equation (45) is only valid at reasonably large pH (see appendix).

Figure 10 demonstrates a considerable range of validity of (45). In Figure 10, $c_{R^0} = 6$ μM throughout, and $\Delta\bar{S}_2$ is constant above about $\bar{c}_H = 10^{-8}$ M. Below this limit the invalidity of $\bar{c}_H >> K_{ER,H}$ becomes quite apparent: ΔS_2 becomes progressively smaller as $\bar{c}_H$ is decreased, which also has an adverse effect on the preciseness with which τ_2 can be determined at this pH. This may be seen in Figure 6. It is interesting that $\Delta\bar{S}_2$ in phosphate is much larger than $\Delta\bar{S}_2$ in glycylglycine, though the latter buffer has a much higher enthalpy of reaction then the former. Assuming that the values indicated in Figure 10 by the arrow ($\Delta\bar{S}_P = 30$ mv in phosphate, $\Delta\bar{S}_G = 20$ mv in glycylglycine) are limits, one obtains with $(\Sigma\Delta H)_P$ = effective enthalpy in phosphate buffer, $(\Sigma\Delta H)_G$ = effective enthalpy in glycylglycine buffer, the quotient

$$\frac{\Delta\bar{S}_P}{\Delta\bar{S}_G} = \frac{(\Sigma\Delta H)_P}{(\Sigma\Delta H)_G} = \frac{3}{2} \qquad (46)$$

since only the sum of the enthalpies may be considered buffer-dependent. Here (46) gives with (A 68) and rearrangement:

$$\Delta H_{ER,H} + \Delta H_{E,R} = 3\Delta H_{G,H} - 2\Delta H_{P,H} \qquad (47)$$

One obtains from the literature (25°):

$\Delta H_{P,H} = -0.9$ kcal/mole for phosphate
(Bates and Acree, 1945)

$\Delta H_{G,H} = -10.0$ kcal/mole for glycylglycine
(Cohn and Edsall, 1943)

Thus, $\Delta H_{ER,H} + \Delta H_{E,R} = -30 + 1.8$ kcal/mole $= -28.2$ kcal/mole. Such an enthalpy for $\Delta H_{ER,H} + \Delta H_{E,R}$ is certainly surprisingly high. But the error in it is very large and the value may be -20 kcal/mole. A more precise value could only be obtained after considerable refinement of the experiments.

The experimental data in Figure 11 are scattering little from a straight line for pH ≤ 8, which is in agreement with the results from Figure 10. A strong deviation becomes apparent for $\bar{c}_H = 10^{-9}$ M (as in Figure 10). The experimental values demonstrate again the steepest slope in phosphate at pH 7 because of the largest $\Sigma\Delta H$. But the data in glycylglycine are slightly higher at pH 7 than at pH 8. This only means that deviations from (A 70) become in reality already apparent at $\bar{c}_H = 10^{-8}$ M.

DISCUSSION

The most extensive recent investigation on the malate dehydrogenase system relevant to this present investigation is the work of Raval and Wolfe (1962a). They give in their Table III at various pH values a number of velocity constants for recombination and dissociation of ER, as derived from over-all reaction kinetics. Here k_8 is their bimolecular velocity constant for the formation of ER and stays relatively unchanged. Their monomolecular velocity constant for the disso-

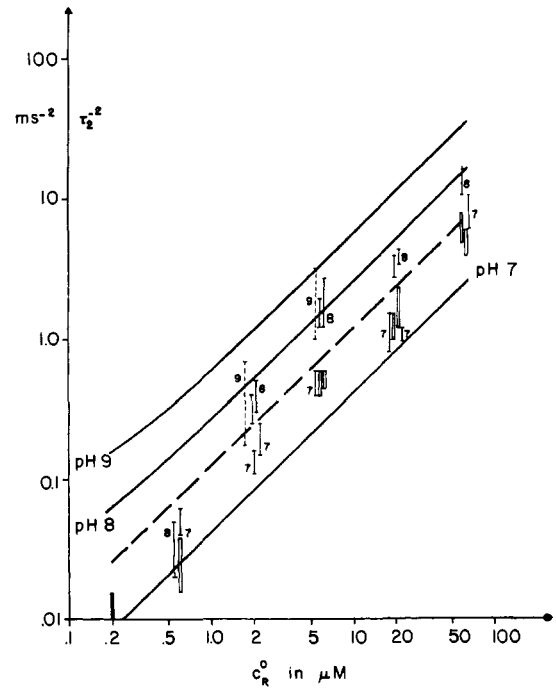

FIG. 9.—Plot of τ_2^{-2} as a function of c_{R^0} at various pH values. The theoretical lines were drawn in with equation (38) and the parameters were obtained from earlier experiments. The strong dashed line refers to phosphate pH 7, while the solid long lines refer to glycylglycine (at indicated pH). The boxes represent systems in phosphate at pH 7, while the vertical lines indicate glycylglycine as buffer, but for better discrimination, the data at pH 9 have been shown as dashed lines. The numbers near the vertical lines indicate pH values.

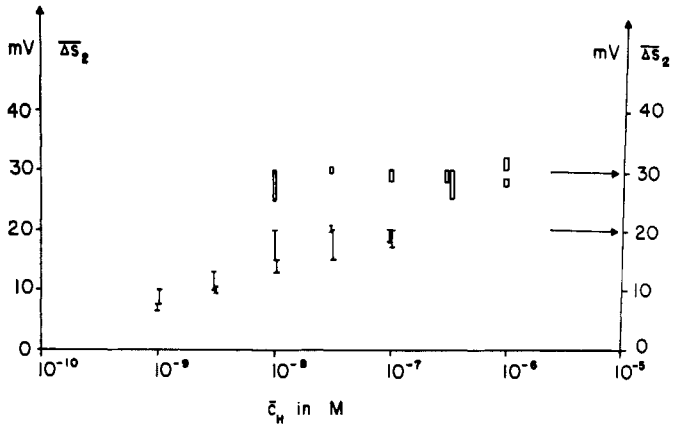

FIG. 10.—A plot of the height of chemical relaxation $\Delta\bar{S}$ as a function of $\bar{c}_H$. Boxes indicate measurements in phosphate, lines those in glycylglycine. Conditions are otherwise as for Figure 5.

TABLE I
COMPARISON OF KINETIC CONSTANTS

*p*H	k_7 (sec^{-1})	k_2' (sec^{-1})	k_2'' (sec^{-1})	k_8 M^{-1} sec^{-1}
6.0	50	1.7	5	$1.0 \cdot 10^7$
7.0	83	16	45	$2.3 \cdot 10^7$
8.0	167	100	167	$3.3 \cdot 10^7$
9.0	250	210	230	$2.8 \cdot 10^7$
10.0	800	240	240	$1.6 \cdot 10^7$

[a] Comparison of kinetic constants obtained in this investigation with those from the literature. Here k_7 and k_8 were derived from Table III of Raval and Wolfe (1962a) and are the velocity constants for dissociation and association, respectively, of the DPNH-enzyme complexes, as obtainable from steady-state kinetics. Also k_2 is a computation of the apparent velocity constant for dissociation according to equation (4) with $k_3 = 240$ sec^{-1}. Here k_2' refers to glycylglycine, and k_2'' to phosphate as buffer; k_7 and k_8 were measured in Tris-acetate buffer.

ciation of ER varies considerably between *p*H 6 and 10. In the trend of change it would correspond to the *p*H-dependent velocity constant k_2 of equation (9), as defined by equation (40). Table I gives a comparison of the data from the literature with the data from this investigation. There is reasonable agreement at *p*H values 8 and 9. The deviations at the lower *p*H values are understandable, as equation (40) no longer holds (as explained in the Appendix). The deviation at *p*H 10 might be due to another protonic dissociation.

While agreement between the monomolecular constant may be considered satisfactory, there are considerable discrepancies in the values for the bimolecular velocity constant which was found to be 6.8×10^8 sec^{-1} M^{-1} in this investigation. This is more than a magnitude above the value of Raval and Wolfe. One reason for this discrepancy may be sought in the type of enzyme. The enzyme used in this investigation was commercial grade treated only by dialysis, while Raval and Wolfe (1962b) used chromatography. According to a personal communication by R. T. Wolfe, they used only one isozyme of this enzyme. It seems that the mixture of isozymes demonstrates its effect only on the bimolecular constant. It might be mentioned at this occasion that differences in the bimolecular velocity constant were observed from sample to sample, which varied from as much as 1.5×10^8 to 6.8×10^8 $sec^{-1}M^{-1}$; a change in the apparent monomolecular velocity constant was associated with this; it varied from 22 sec^{-1} to 100 sec^{-1} (both at *p*H 7, phosphate buffer). Another reason for the differences in the data of Raval and Wolfe and ours might be sought in the different buffers —Raval and Wolfe used Tris-acetate.

The data derived from thermodynamics and kinetics of chemical relaxation demonstrate considerable scattering and a rather large error. This may partially be due to the mixture of isozymes. Another reason is apparent from Figure 1, which shows that there is initially a very fast change in the fluorescence followed by the slow chemical relaxation. As the onset of this relaxation is important for determining the total change of the signal due to chemical relaxation and the relaxation time, it is important to open up the electronic filter of the detection system very much further than would be necessary only to obtain an ordinary relaxation curve. In the latter case, the electronic time constant would only have to be one-tenth of the chemical relaxation time. In these experiments the time constant of the electronic filter had to be diminished by a factor of up to 100. A fast electronic switching circuit is in development to circumvent this problem.

It is apparent that these results can only be considered preliminary and should be repeated under improved conditions, considering the foregoing aspects. So far only one protonic dissociation and one combination of DPNH with an enzyme species was considered, leading to a satisfactory interpretation of the experimental results. Raval and Wolfe (1962a) report four protonic dissociations and three combinations of DPNH with three different protonic species of the enzyme in their Figure 3. The presence of such a large number of species can not be concluded from these experiments, but later investigations with considerably increased refinement may reveal the participation of more than one protonic dissociation constant. For this purpose, it would be necessary to scan a considerably wider *p*H range than was done in this investigation. In order to circumvent slow degradation processes, a stopped-flow system would possibly have to be used at the extreme *p*H ranges. While the present data showed degradation phenomena already appearing at *p*H 6, the small jump height $\Delta\bar{S}_2$ may cause considerable difficulties in the determination of relaxation times at high *p*H (see Figures 8 and 10).

Generally it may be concluded that chemical relaxation permits one to directly investigate the kinetics of fast biological reactions independently from and more directly than steady-state kinetics. Thus, the discrepancies between k_8 in Table I (obtained from over-all reaction kinetics) and the bimolecular velocity constant obtained from this investigation may have its origin in some "hidden" equilibrium constant which cannot be separated from k_8 when derived from steady-state kinetics. Here $k_4 > k_8$ is in agreement with the careful analysis on systems with multiple intermediates

under steady-state conditions, which has recently been published by Bloomfield *et al.* (1962a). Certainly, substrate activation might also lead to a small value of k_3. It is expected that future work of the application of the temperature-jump method to the malate dehydrogenase system would lead to a clarification of these differences.

Appendix

Statics.—The chemical part of the fluorescence signal $S_T - S_0$ is to be expressed in terms of the analytical concentrations c_R^0 and c_E^0; the conditions given by the buffer are expressed in terms of the hydrogen-ion concentration $\bar{c}_H$. For the system given by equation (13),

$$S_T - S_0 = \eta_R \bar{c}_R + \eta_{ER} \bar{c}_{ER} + \eta_{ERH} \bar{c}_{ERH} \quad (A\ 1)$$

A term with $\bar{c}_E$ can be neglected, as the molar fluorescence coefficient of E, η_E, is comparatively very small under the spectral conditions of the experiment. The directly accessible analytical concentrations are connected to the equilibrium concentrations by

$$c_R^0 = \bar{c}_R + \bar{c}_{ER} + \bar{c}_{ERH} \quad (A\ 2)$$

$$c_E^0 = \bar{c}_E + \bar{c}_{ER} + \bar{c}_{ERH} \quad (A\ 3)$$

These equations allow, on one hand, reformulation of (A 1):

$$S_T - S_0 = \eta_R c_R^0 + (\eta_{ER} - \eta_R)\bar{c}_{ER} + (\eta_{ERH} - \eta_R)\bar{c}_{ERH} \quad (A\ 4)$$

On the other hand, they allow (with the use of equations 32 and 33) the expression of the equilibrium concentrations in terms of analytical concentrations. With the experimental condition $c_E^0 = c_R^0$, one finally obtains

$$\bar{c}_{ER} = \left\{c_R^0 + \frac{K_{E,R}}{2}\left(1 + \frac{\bar{c}_H}{K_{ER,H}}\right)^{-1}\right\}\left(1 + \frac{\bar{c}_H}{K_{ER,H}}\right)^{-1} \cdot \left\{1 - \left[1 - \left\langle 1 + \frac{K_{E,R}}{2c_R^0}\left(1 + \frac{\bar{c}_H}{K_{ER,H}}\right)^{-1}\right\rangle^{-2}\right]^{1/2}\right\} \quad (A\ 5)$$

$$\bar{c}_{ERH} = \left\{c_R^0 + \frac{K_{E,R}}{2}\left(1 + \frac{\bar{c}_H}{K_{ER,H}}\right)^{-1}\right\}\left(1 + \frac{K_{ER,H}}{\bar{c}_H}\right)^{-1} \cdot \left\{1 - \left[1 - \left\langle 1 + \frac{K_{E,R}}{2c_R^0}\left(1 + \frac{\bar{c}_H}{K_{ER,H}}\right)^{-1}\right\rangle^{-2}\right]^{1/2}\right\} \quad (A\ 6)$$

and

$$\bar{c}_R = \frac{1}{2} K_{E,R} \frac{K_{ER,H}}{K_{ER,H} + \bar{c}_H}\left\{\left[1 + \frac{4c_R^0}{K_{E,R}} \cdot \frac{K_{ER,H} + \bar{c}_H}{K_{ER,H}}\right]^{1/2} - 1\right\} \quad (A\ 7)$$

Equation (A 5) and (A 6) are equal except for one factor in brackets. Inserting these equations into (A 4) therefore gives

$$S_T - S_0 = \eta_R \bar{c}_R^0 + \left\{(\eta_{ER} - \eta_R)\frac{K_{ER,H}}{K_{ER,H} + \bar{c}_H} + (\eta_{ERH} - \eta_R)\frac{\bar{c}_H}{K_{ER,H} + \bar{c}_H}\right\} \cdot c_R^0 \left\{1 + \frac{K_{E,R}}{2c_R^0} \cdot \frac{K_{ER,H}}{K_{ER,H} + c_H}\right\} \left\{1 - \left[1 - \left\langle 1 + \frac{K_{E,R}}{2c_R^0} \cdot \frac{K_{ER,H}}{K_{ER,H} + \bar{c}_H}\right\rangle^{-2}\right]^{1/2}\right\} \quad (A\ 8)$$

Dividing both sides of the equation by $\eta_R c_R^0$ gives equation (41) of the main text with definitions (42) to (44). Introducing the complex equilibrium constant K_0 according to (31) gives equation (30) of the main text. Equation (34) is obtained from (A 5) by introducing this same constant K_0.

Kinetics.—Relations between the observable relaxation times τ and the kinetic parameters of the system have to be found. The differential equations for system (13) are:

$$\frac{dc_{ERH}}{dt} = -k_1 c_{ERH} c_B + k_2 c_{ER} c_{BH} \quad (A\ 9)$$

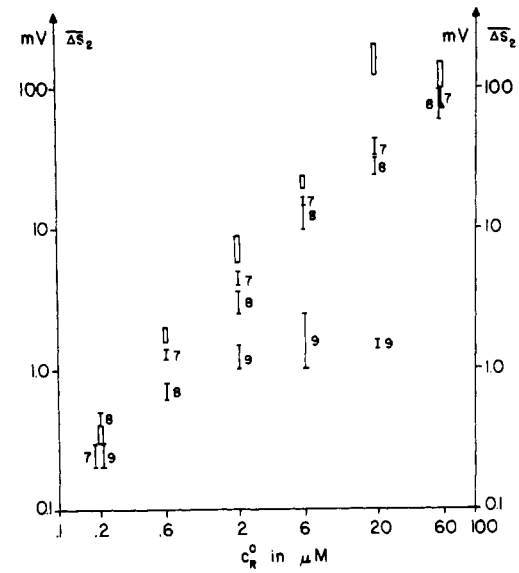

FIG. 11.—The signal change due to chemical relaxation, $\Delta\bar{S}$, is plotted as a function of the total analytical concentration of DPNH, c_R^0. Boxes indicate phosphate buffer at *p*H 7. Otherwise the lines indicate glycylglycine, with the numbers near the lines giving the *p*H values.

$$\frac{dc_R}{dt} = +k_3 c_{ER} - k_4 c_E c_R \quad (A\ 10)$$

The arbitrary (time-dependent) concentration c_Y may be expressed in terms of the (time-independent) equilibrium concentration $\bar{c}_Y$ and the time-independent deviation from this equilibrium value, Δc_Y:

$$c_Y = \bar{c}_Y + \Delta c_Y \quad (A\ 11)$$

The conditions of chemical relaxation establish:

$$\bar{c}_Y \gg \Delta c_Y \quad (A\ 12)$$

With $d\bar{c}_Y/dt = 0$ and $\Delta c_Y \Delta c_Z \to 0$ (Z generally different from Y), one obtains

$$\frac{d\ \Delta c_{ERH}}{dt} = -k_1(\bar{c}_{ERH}\ \Delta c_B + \bar{c}_B\ \Delta c_{ERH}) + k_2(\bar{c}_{ER}\ \Delta c_{BH} + \bar{c}_{BH}\ \Delta c_{ER}) \quad (A\ 13)$$

$$\frac{d\ \Delta c_R}{dt} = +k_3\ \Delta c_{ER} - k_4(\bar{c}_E\ \Delta c_R + \bar{c}_R\ \Delta c_E) \quad (A\ 14)$$

From stoichiometry and conservation of mass one obtains the relationships

$$\Delta c_B = \Delta c_{ERH} \quad (A\ 15)$$

$$\Delta c_{BH} = -\Delta c_{ERH} \quad (A\ 16)$$

$$\Delta c_E = \Delta c_R \quad (A\ 17)$$

$$\Delta c_{ER} = -\Delta c_{ERH} - \Delta c_R \quad (A\ 18)$$

Inserting these relationships into (A 13) and (A 14) gives

$$\frac{d\ \Delta c_{ERH}}{dt} = -a_{11}\ \Delta c_{ERH} - a_{12}\ \Delta c_R \quad (A\ 19)$$

$$\frac{d\ \Delta c_R}{dt} = -a_{21}\ \Delta c_{ERH} - a_{22}\ \Delta c_R \quad (A\ 20)$$

with

$$a_{11} = k_1(\bar{c}_{ERH} + \bar{c}_B) + k_2(\bar{c}_{ER} + \bar{c}_{BH}) \quad (A\ 21)$$

$$a_{12} = k_2 \bar{c}_{BH} \quad (A\ 22)$$

$$a_{21} = k_3 \quad (A\ 23)$$

$$a_{22} = k_3 + k_4(\bar{c}_E + \bar{c}_R) \quad (A\ 24)$$

The solution of the two homogeneous linear differential

equations of first order is given[5] by

$$\Delta c_{ERH} = A_{11} \exp(-t/\tau_1) + A_{12} \exp(-t/\tau_2) \quad (A\ 25)$$

$$\Delta c_R = A_{21} \exp(-t/\tau_1) + A_{22} \exp(-t/\tau_2) \quad (A\ 26)$$

The concentration coefficients A_{ij} will not be considered now as they deal with equilibrium changes, to be treated in the next section. There is one other equation of this type which needs to be considered later, namely,

$$\Delta c_{ER} = A_{31} \exp(-t/\tau_1) + A_{32} \exp(-t/\tau_2) \quad (A\ 27)$$

Here in kinetics, only expressions for the time constants have to be found. Such expressions are obtained from the solution of the determinant

$$\begin{vmatrix} a_{11} - \tau^{-1} & a_{12} \\ a_{21} & a_{22} - \tau^{-1} \end{vmatrix} = 0 \quad (A\ 28)$$

Its general solution is

$$(\tau_{1,2})^{-1} = \frac{a_{11} + a_{22}}{2} \{1 \pm [1 - b]^{1/2}\} \quad (A\ 29)$$

where

$$b = \frac{4(a_{11}a_{22} - a_{12}a_{21})}{(a_{11} + a_{22})^2} \quad (A\ 30)$$

a_{11}^{-1} and a_{22}^{-1} are the "EINZEL"-relaxation times (the "STEP"-relaxation times) attributable to individual reaction steps and for their definition to be considered isolated from other reactions. To determine two relaxation times under ordinary signal-to-noise conditions as individual entities, they must be separated by at least one order of magnitude (under favorable conditions, otherwise (and more frequently) by a factor of 30 or even by two orders of magnitude, see Figure 2). The system under consideration has also two steps of highly different speed. The slow step is, under experimental conditions (Figure 4), never faster than about 500 μsec (this is the slow *over-all* step, introduced as τ_2 below). The experiments permit one only to estimate an upper limit of the proton-transferring fast step which is around 50 μsec (see also below). Then the following condition would hold:

$$a_{11} \gg a_{22} \quad (A\ 31)$$

Conditions as given by (A 31) are very important for a simplified treatment of kinetics of chemical relaxation: one realizes immediately that (A 30) becomes with (A 31):

$$b = 4\left(\frac{a_{22}}{a_{11}} - \frac{a_{12}}{a_{11}} \cdot \frac{a_{21}}{a_{11}}\right) \quad (A\ 32)$$

A look at the structure of the coefficient a_{ij} (equations A 21 to A 24) demonstrates immediately that $a_{11} > a_{12}$ and $a_{22} > a_{21}$. Thus it is for sufficiently large separation according to (A 31):

$$1 \gg b > 0 \quad (A\ 33)$$

which immediately allows one to write the two roots of (A 29) explicitly:

$$\tau_1^{-1} = a_{11} \quad (A\ 34)$$

or with (A 21):

$$\tau_1^{-1} = k_1(\bar{c}_{ERH} + \bar{c}_B) + k_2(\bar{c}_{ER} + \bar{c}_{BH}) \quad (A\ 35)$$

[5] The structure of (A 25) to (A 27) implies an arrangement of the integration limits, which considers the final equilibrium values at 25° as "zero-position." This was already explicitly demonstrated by Figure 3 and its associated equation (3). It will be treated further in the Appendix section on Thermodynamics.

and

$$\tau_2^{-1} = a_{22} - \frac{a_{12}}{a_{11}} a_{21} \quad (A\ 36)$$

or with (A 21) to (A 24):

$$\tau_2^{-1} = k_3\left(1 - \frac{k_2\bar{c}_{BH}}{k_1(\bar{c}_{ERH} + \bar{c}_B) + k_2(\bar{c}_{ER} + \bar{c}_{BH})}\right) + k_4(\bar{c}_E + \bar{c}_R) \quad (A\ 37)$$

Under "ordinary" conditions of the experiment,

$$\bar{c}_B, \bar{c}_{BH} \gg \bar{c}_E, \bar{c}_{ER}, \bar{c}_{ERH} \quad (A\ 38)$$

With this additional experimental condition, one obtains from (A 35):

$$\tau_1^{-1} = k_1\bar{c}_B + k_2\bar{c}_{BH} \quad (A\ 39)$$

and from (A 37), after rearrangement and use of (33) of the main text:

$$\tau_2^{-1} = k_3(1 + \bar{c}_H/K_{ER,H})^{-1} + k_4(\bar{c}_E + \bar{c}_R) \quad (A\ 40)$$

With (A 2) and (A 3), the former experimental condition $c_E^0 = c_R^0$ leads to $\bar{c}_E = \bar{c}_R$, so that

$$\tau_2^{-1} = k_3 \frac{K_{ER,H}}{K_{ER,H} + \bar{c}_H} + 2k_4\bar{c}_R \quad (A\ 41)$$

One may now substitute the expression (A 7) for $\bar{c}_R$ and incorporate $K_{E,R} = k_3/k_4$ (compare (32) and the definition of $K_{i,i+1}$ similar to (17)).

After some rearrangement one obtains upon squaring:

$$\tau_2^{-2} = \left(k_3 \frac{K_{ER,H}}{K_{ER,H} + \bar{c}_H}\right)^2 \left[1 + \frac{4c_R^0}{K_{E,R}} \cdot \frac{K_{ER,H} + \bar{c}_H}{K_{ER,H}}\right] \quad (A\ 42)$$

Multiplying out gives an expression which at constant $\bar{c}_H$ is a linear function of the analytical concentration c_R^0:

$$\tau_2^{-2} = \left(k_3 \frac{K_{ER,H}}{K_{ER,H} + \bar{c}_H}\right)^2 + 4c_R^0k_4 \left(k_3 \frac{K_{ER,H}}{K_{ER,H} + \bar{c}_H}\right) \quad (A\ 43)$$

A linear plot gives the first term as intersection with the ordinate, while the intersection with the abscissa leads to

$$-c_R^0 = \frac{1}{4} K_{E,R} \frac{K_{ER,H}}{K_{ER,H} + \bar{c}_H} \quad (A\ 44)$$

Unfortunately, the large range in c_R^0 to be covered and the squaring of the reciprocal time constants make an evaluation of this type somewhat difficult, and especially so since $K_{E,R}$ is comparatively small to the values of c_R^0 used in these experiments. Such an evaluation could therefore not be made with the experimental results of this investigation.

Relation (A 38) may no longer be fulfilled at very low and very high $\bar{c}_H$. Here $\bar{c}_{BH}$ is very small at very low $\bar{c}_H$, so that, if $k_1 \approx k_2$ (which may be assumed approximately), $k_1\bar{c}_B >> k_2\bar{c}_{BH}$, by which (A 37) simplifies to

$$\tau_2^{-1} = k_3 + k_4(\bar{c}_E + \bar{c}_R) \quad (A\ 45)$$

This is the same expression to which (A 40) simplifies for $K_{ER,H} >> \bar{c}_H$.

At very high $\bar{c}_H$, $\bar{c}_{BH}$ is very large and $\bar{c}_{ER}$ extremely small. Thus equation (A 37) becomes (incorporating $\bar{c}_E = \bar{c}_R$):

$$\tau_2^{-1} = k_3 \frac{k_1(\bar{c}_{ERH} + \bar{c}_B)}{k_2\bar{c}_{BH}} + 2k_4\bar{c}_R \quad (A\ 46)$$

One realizes for the second term in (A 46) that it approaches zero upon substitution of $\bar{c}_R$ by (A 7), with

increasing $\bar{c}_H$. But also for very large $\bar{c}_H$, $\bar{c}_{ERH} \rightarrow c_R^0$ and $\bar{c}_{BH} \rightarrow c_B^0$, so that

$$\tau_2^{-1} \rightarrow k_3 \frac{K_{ER,H}}{K_{B,H}} \cdot \frac{c_R^0}{c_B^0} \qquad \text{(A 47)}$$

For glycylglycine as buffer, $K_{B,H} \approx 10^{-8}$, so that $K_{1,2} = K_{ER,H}K_{B,H}^{-1} \approx 1$. In the experiment of Figure 4, $c_R^0 = 6 \cdot 10^{-6}$ M and $c_B^0 = 4.6 \cdot 10^{-3}$ M. Thus, at very high $\bar{c}_H$

$$\tau_2^{-1} \longrightarrow k_3 \times 1.3 \times 10^{-3} = 0.31 \text{ sec}^{-1}$$

This limiting value is only of theoretical interest, as a buffer can no longer be considered in its buffer range when $c_R^0 > \bar{c}_B$. Even much before $c_R^0 = c_B^0$ is reached, it is expected that self-buffering of the enzyme moiety sets in. This would add further demands to $\bar{c}_{ERH}$ in (A 46), leading to a much larger limiting value for τ_2^{-1} than derivable from (A 47). A quantitative expression for this limit cannot be given until one knows the details of the protonic dissociation constants of the enzyme. It is also possible that dissolved CO_2 could act as buffer, but it could be excluded by the use of N_2.

Thermodynamics.—The change in fluorescence due to *chemical relaxation* is given by

$$\Delta S_T = \Delta S_R + \Delta S_{ER} + \Delta S_{ERH} \qquad \text{(A 48)}$$

where each individual ΔS_Y is related to its Δc_Y by

$$\Delta S_Y = \eta_Y \Delta c_Y \qquad \text{(A 49)}$$

Explicit expressions for the three concentration changes Δc_Y have already been given by equations (A 25), (A 26), and (A 27). If the relaxation processes are sufficiently separated, one could distinguish a fast ΔS_1 from a slow ΔS_2 with

$$\Delta S_T = \Delta S_1 + \Delta S_2 \qquad \text{(A 50)}$$

While ΔS_1 contains all terms with τ_1, ΔS_2 contains all terms with τ_2. The latter change is detected in the experiments, so only ΔS_2 may be considered[6] and one obtains, with the above-mentioned equations

$$\Delta S_2 = (\eta_{ERH}A_{12} + \eta_R A_{22} + \eta_{ER}A_{32}) \exp(-t/\tau_2) \qquad \text{(A 51)}$$

The coefficient in front of the exponential term represents the total observable change in fluorescence signal due to chemical relaxation with τ_2; it is $\Delta \bar{S}_2$.

The factors A_{ij} are concentrations and have to be connected to equilibrium concentration changes of the system. For this purpose, one first writes (see equation 33):

$$K_{2,1} = \frac{\bar{c}_B \bar{c}_{ERH}}{\bar{c}_{BH} \bar{c}_{ER}} \qquad \text{(A 52)}$$

Employing $K_{2,1} >> \Delta K_{2,1}$ and $c_Y >> \Delta c_Y$ (see A 12), one may write

$$\frac{\Delta K_{2,1}}{K_{2,1}} = \frac{\Delta \bar{c}_B}{\bar{c}_B} + \frac{\Delta \bar{c}_{ERH}}{\bar{c}_{ERH}} - \frac{\Delta \bar{c}_{BH}}{\bar{c}_{BH}} - \frac{\Delta \bar{c}_{ER}}{\bar{c}_{ER}} \qquad \text{(A 53)}$$

Similarly, one obtains from equation (32):

$$\frac{\Delta K_{4,3}}{K_{4,3}} = \frac{\Delta \bar{c}_{ER}}{\bar{c}_{ER}} - \frac{\Delta \bar{c}_E}{\bar{c}_E} - \frac{\Delta \bar{c}_R}{\bar{c}_R} \qquad \text{(A 54)}$$

For the fast relaxation process one has to use only (A 53) to solve for the individual $(\Delta \bar{c}_Y)_1$. As $\Delta \bar{c}_R$ does not appear in (A 53), $(\Delta \bar{c}_R)_1 = 0$. Otherwise, one has the interrelationship

$$(\Delta \bar{c}_{ERH})_1 = (\Delta \bar{c}_B)_1 = -(\Delta \bar{c}_{BH})_1 = -(\Delta \bar{c}_{ER})_1 \qquad \text{(A 55)}$$

which together with

$$\frac{\Delta \bar{c}_{ERH}}{\bar{c}_{ERH}}, \frac{\Delta \bar{c}_{ER}}{\bar{c}_{ER}} \gg \frac{\Delta \bar{c}_B}{\bar{c}_B}, \frac{\Delta \bar{c}_{BH}}{\bar{c}_{BH}} \qquad \text{(A 56)}$$

results in

$$\frac{(\Delta \bar{c}_{ERH})_1}{\bar{c}_{ERH}} = \frac{\frac{\Delta K_{B,H}}{K_{B,H}} - \frac{\Delta K_{ER,H}}{K_{ER,H}}}{1 + \bar{c}_H/K_{ER,H}} \qquad \text{(A 57)}$$

and

$$\frac{(\Delta \bar{c}_{ER})_1}{\bar{c}_{ER}} = \frac{\frac{\Delta K_{ER,H}}{K_{ER,H}} - \frac{\Delta K_{B,H}}{K_{B,H}}}{1 + K_{ER,H}/\bar{c}_H} \qquad \text{(A 58)}$$

For the total change involving both relaxation times τ_1 and τ_2, the combination of equations (A 53) and (A 54) leads to the individual changes of equilibrium concentrations. The interrelationships among the $(\Delta \bar{c}_Y)_2$ terms are then (similar to A 15 to A 18):

$$(\Delta \bar{c}_{ERH})_2 = (\Delta \bar{c}_B)_2 = -(\Delta \bar{c}_{BH})_2 \qquad \text{(A 59)}$$

$$(\Delta \bar{c}_R)_2 = (\Delta \bar{c}_E)_2 \qquad \text{(A 60)}$$

$$(\Delta \bar{c}_{ER})_2 = -(\Delta \bar{c}_R)_2 - (\Delta \bar{c}_{ERH})_2 \qquad \text{(A 61)}$$

Using these relationships together with (A 56) and solving for the three concentration changes gives:

$$\frac{(\Delta \bar{c}_{ERH})_2}{\bar{c}_{ERH}} = \frac{\frac{\Delta K_{B,H}}{K_{B,H}} - \frac{\Delta K_{ER,H}}{K_{ER,H}} - \frac{\Delta K_{E,R}}{K_{E,R}} + \left(\frac{\Delta K_{B,H}}{K_{B,H}} - \frac{\Delta K_{ER,H}}{K_{ER,H}}\right) 2K_{E,R}^{-1}\bar{c}_R}{1 + \left(1 + \frac{\bar{c}_H}{K_{ER,H}}\right)\frac{2\bar{c}_R}{K_{E,R}}} \qquad \text{(A 62)}$$

$$\frac{(\Delta \bar{c}_{ER})_2}{\bar{c}_{ER}} = \frac{\left(\frac{\Delta K_{B,H}}{K_{B,H}} - \frac{\Delta K_{ER,H}}{K_{ER,H}}\right)\frac{\bar{c}_H}{K_{ER,H}} \cdot \frac{2\bar{c}_R}{K_{E,R}} + \frac{\Delta K_{E,R}}{K_{E,R}}}{1 + \left(1 + \frac{\bar{c}_H}{K_{ER,H}}\right)\frac{2\bar{c}_R}{K_{E,R}}} \qquad \text{(A 63)}$$

$$\frac{(\Delta \bar{c}_R)_2}{\bar{c}_R} = \frac{\frac{\Delta K_{ER,H}}{K_{ER,H}} - \frac{\Delta K_{B,H}}{K_{B,H}} + \frac{\Delta K_{E,R}}{K_{E,R}}\left(1 + \frac{K_{ER,H}}{\bar{c}_H}\right)}{2 + \frac{K_{ER,H}}{\bar{c}_H}\left(1 + \frac{K_{E,R}}{2\bar{c}_R}\right)} \qquad \text{(A 64)}$$

The individual concentration factors A_{ij} of (A 51), referring all to the slow relaxation process with τ_2, are then:

$$A_{12} = (\Delta \bar{c}_{ERH})_2 - (\Delta \bar{c}_{ERH})_1 \qquad \text{(A 65)}$$

$$A_{22} = (\Delta \bar{c}_R)_2 - (\Delta \bar{c}_R)_1 \qquad \text{(A 66)}$$

$$A_{32} = (\Delta \bar{c}_{ER})_2 - (\Delta \bar{c}_{ER})_1 \qquad \text{(A 67)}$$

Thus, $\Delta \bar{S}_2$ becomes an extremely complex expression, since at least two of the equations (A 5), (A 6), and (A 7) must be incorporated. But a crude estimate can be made, especially since the results are rather crude in themselves and do not warrant precise description.

The main fluorescence signal comes from ERH (as "approximately" $\eta_{ERH} >> \eta_{ER}, \eta_R$). At high $\bar{c}_H$, therefore, only A_{12} may be considered. At high $\bar{c}_H$ almost all DPNH is bound to enzyme, so that one may assume here $K_{E,R} >> 2\bar{c}_R$, which in turn shortens the numerator of (A 62). At high $\bar{c}_H$, $\bar{c}_H >> K_{ER,H}$ also, which leads to a very small expression for (A 57). The diminishing effect of $\bar{c}_H$ in the denominator of (A 62) is partly compensated by the factor $2\bar{c}_R/K_{E,R}$ (compare with A 7), so that $(\Delta \bar{c}_{ERH})_1$ may be neglected compared to $(\Delta \bar{c}_{ERH})_2$. Thus, $\Delta \bar{S}_2 \approx \eta_{ERH}(\Delta \bar{c}_{ERH})_2$.

[6] This actually means, with respect to Figure 1, that the initial step before the visible relaxation process contains both $\Delta \bar{S}_0$ and $\Delta \bar{S}_1$ (no dependence upon time is assumed to be left in the observation range of τ_2).

Inserting $(1 + p)$ for the denominator of (A 62) and using

$$\Sigma\Delta H = \Delta H_{E,H} - \Delta H_{ER,H} - \Delta H_{E,R} \quad \text{(A 68)}$$

and

$$\frac{\Delta K_{Y,Z}}{K_{Y,Z}} = \frac{\Delta H_{Y,Z}}{RT^2} \quad \text{(A 69)}$$

leads to

$$\frac{(\Delta \bar{c}_{ERH})_2}{\bar{c}_{ERH}} \approx \frac{\Sigma\Delta H}{1 + p} \frac{\Delta T}{RT^2} \quad \text{(A 70)}$$

This last equation may be used for a crude relative evaluation of enthalpies as demonstrated in the main part under Thermodynamics.

Acknowledgments

The authors would like to express their high appreciation to Dr. Britton Chance for his continuous stimulating interest in the progress of this investigation. They would also like to thank Miss Johanna Schwartz and Mr. Albrecht Foelsing for their assistance in checking the derivations of the equations and in the numerical evaluations.

References

Bates, R. G., and Acree, S. F. (1945), *J. Res. Nat. Bur. Std. 34*, 373.

Bloomfield, V., Peller, L., and Alberty, R. A. (1962a), *J. Am. Chem. Soc. 84*, 4367.

Bloomfield, V., Peller, L., and Alberty, R. A. (1962b), *J. Am. Chem. Soc. 84*, 4375.

Cohn, E. J., and Edsall, J. T. (1943), Proteins, Amino Acids and Peptides, New York, Reinhold, p. 89.

Czerlinski, G. (1958), Ph.D. dissertation, University of Göttingen.

Czerlinski, G., and Eigen, M. (1959), *Z. Elektrochem. 63*, 652.

Czerlinski, G. (1962), *Rev. Sci. Instr. 33*, 1184.

Czerlinski, G., and Schreck, G. (1964), *J. Biol. Chem. 239* (in press).

Eigen, M. (1954), *Discussions Faraday Soc. 17*, 194.

Eigen, M., and De Maeyer, L. (1963), *in* Technique of Organic Chemistry, 2nd ed., Vol. VIII, Weissberger, A., ed., New York, Interscience, part 2, p. 895, a general treatment of chemical relaxation.

Kornberg, A. (1953), *Biochem. Prep. 3*, 20.

Ochoa, S. (1955), *in* Methods in Enzymology, Vol. I, Colowick, S. P., and Kaplan, N. O., eds., New York, Academic, p. 735.

Peller, L., and Alberty, R. A. (1959), *J. Am. Chem. Soc. 81*, 5907.

Raval, D. N., and Wolfe, R. G. (1962a), *Biochemistry 1*, 1118.

Raval, D. N., and Wolfe, R. G. (1962b), *Biochemistry 1*, 263.

Roughton, F. J. W., and Chance, B. (1963), *in* Technique of Organic Chemistry, 2nd ed., Vol. VIII, Weissberger, A., ed., New York, Interscience, part 2, pp. 704 ff., 1231 ff.

Theorell, H., and Langan, T. A. (1960), *Acta Chem. Scand. 14*, 933.

Theorell, H., and McKinley-McKee, H. S. (1961), *Acta Chem. Scand. 15*, 1811.

Experiments on the Mechanism of Gramicidin and Tyrocidine Synthesis in Cell-free Preparations of *Bacillus brevis**

K. Okuda,† I. Uemura,† J. W. Bodley,‡ and T. Winnick

From the Department of Biochemistry and Biophysics, University of Hawaii, Honolulu

Received August 1, 1963

Studies have been made of the mechanism of biosynthesis of the gramicidin and tyrocidine polypeptides, with ribosomes and various soluble preparations, derived from sonic extracts of *Bacillus brevis*. The pathway of L-amino acid utilization appeared to proceed through the following stages: activation via the adenylate, incorporation into soluble RNA, and transfer from aminoacyl-s-RNA to ribosomes. While D-amino acids were readily activated, they were poorly incorporated into s-RNA, and the possibility of an alternate type of carrier for these D-isomers was explored. Experiments with mixed fractions from two different strains of *B. brevis* revealed that a soluble factor, distinct from amino acid–activating enzymes and from phenol-extractable RNA, controlled the specificity of polypeptide synthesis.

There is now a strong body of evidence in support of the pathway of protein biosynthesis formulated by Zamecnik (1962). By contrast, no requirement has been established for soluble[1] RNA or ribosomes in the formation of glutathione (Lane and Lipmann, 1961), uridine nucleotide peptide (Strominger, 1962), or γ-glutamyl polypeptide (Leonard and Housewright, 1963).

* Supported by a research grant (GM-09335) from the National Institutes of Health, U. S. Public Health Service. Contribution No. 005 from the Pacific Biomedical Research Center, University of Hawaii.

† On leave of absence from the Osaka City University Medical School, Osaka, Japan.

‡ Research performed in partial fulfillment of requirements for the degree of Doctor of Philosophy in Biochemistry, University of Hawaii.

[1] This term is used for convenience, to refer to the RNA possessing both amino acid "acceptor" and "transfer" functions.

The cyclic polypeptides with antibiotic properties, found in a variety of microorganisms, provide additional attractive model systems for the study of mechanisms of peptide-bond synthesis. Two papers (Uemura *et al.*, 1963; Okuda *et al.*, 1963b) dealing with cell-free preparations from *Bacillus brevis* (Dubos-Hotchkiss strain) have revealed that the process of gramicidin and tyrocidine biosynthesis resembles protein synthesis in its requirement for both particulate and soluble cellular components, and in its dependence on ATP, magnesium ions, glutathione, and an amino acid mixture. Polypeptide, as well as protein formation was completely inhibited by chloramphenicol and by puromycin. The synthesis of gramicidins and tyrocidines could be measured by incorporation experiments with isotopic L- and D-amino acids, or by a net increase in antibiotic activity. In either case the newly formed peptides were shown to be attached to ribosomes. By employing combinations of ribosomal and supernatant